Supplementary data

1. Literature review of clinical features of *GRIN1* and *GRIN2B*- associated MCD
    a. Supplementary table 1: Clinical and imaging features of patients with variants in *GRIN1*
    b. Supplementary table 2: Clinical and imaging features of patients with variants in *GRIN2B*
    c. Supplementary table 3: Abnormal brain MRI findings in NMDAR MCD patients.

2. Molecular data
    a. Supplementary table 4: ACMG-AMP criteria used to classify the NMDAR variants
    b. Supplementary table 5: *In silico* predictions for the NMDAR missense variants

3. Electrophysiological studies
    a. Methods
    b. Results

4. Neuropathology
    a. Methods
    b. Supplementary table 6: Antibodies used for the study
    c. Supplementary table 7: Comparative semi-quantitative analysis of immunolabelling in the germinative and intermediate zones as well as in the different layers of the frontal cortex of affected and control patients
    d. d. Supplementary figure 1: Main brain macroscopic and histological findings of individual 8

1. **Literature review of clinical features of *GRIN1* and *GRIN2B*- associated MCD**

a. **Supplementary table 1** – Clinical and imaging features of patients with variants in *GRIN1*

	Fry et al. - P1	Fry et al. - P2	Fry et al. - P3	Fry et al. - P4	Fry et al. - P5	Fry et al. - P6	Fry et al. - P7	Fry et al. - P8	Fry et al. - P9	Fry et al. - P10	Fry et al. - P11	Nishimura et al., 2020	P1 (This paper)	P2 (This paper)	P3 (This paper)	P4 (This paper)
Pathogenic variant	c.2021A>T, p.(Asn674Ile)	c.2381G>A, p.(Arg794Gln)	c.1975C>T, p.(Arg659Trp)	c.1940A>G, p.(Tyr647Cys)	c.2365G>A, p.(Asp789Asn)	c.1652T>C, p.(Leu551Pro)	c.1958C>G, p.(Ala653Gly)	c.1949A>T, p.(Asn650Ile)	c.1975C>T, p.(Arg659Trp)	c.2365G>A, p.(Asp789Asn)	c.1658C>T, p.(Ser553Leu)	c.1949A>C, p.(Asn650Thr)	c.1658C>T, p.(Ser553Leu)	c.1972G>T, p.(Asp658Tyr)	c.1957G>A, p.(Ala653Thr)	c.2231G>A, p.(Cys744Tyr)
Microcephaly (at last control)	- 3.6SD	- 5.2 SD	- 7.1 SD	- 1.5 SD	- 6.5 SD	n/a	- 1.6 SD	- 5.7 SD	n/a	- 6.7 SD	- 7.1 SD	- 2.7 SD	- 5.2 SD	- 2 SD	reduced brain weight, -2 SD	n/a (reduced brain weight)
Development	Severe delay	Severe delay	Severe delay	Severe delay	Severe delay	Severe delay	Severe delay	Severe delay	Severe delay	Severe delay	Severe delay	n/a	Severe delay	Severe delay	n/a	n/a
Neurology	Spastic tetraplegia, axial hypotonia	Spastic tetraplegia, axial hypotonia	Spastic tetraplegia, axial hypotonia	Pseudobulbar palsy, hypotonia	Spastic tetraplegia, axial hypotonia	Spastic tetraplegia, axial hypotonia	n/a	Spastic tetraplegia, axial hypotonia	Mild scoliosis	Spastic tetraplegia, axial hypotonia	Spastic tetraplegia, axial hypotonia	n/a	Hypertonia	Hypo- and hypertonia	n/a	n/a
Onset of seizures	6 W	9 M	2 M	3 M	1 W	1 Y	n/a	1 M	5 W	1 M	2 W	Neonatal	Possibly prenatally	4 M	n/a	n/a
Type of seizures	Myoclonic	Generalized tonic-clonic	Spasms	Tonic	Grimacing	Spasms	n/a	Tonic	Tonic	Gaze deviaition	Tonic	Focal	n/a	Absences, drops, tonic extensions	n/a	n/a
Cortical visual impairment	Yes	Yes	Yes	Yes	Yes	Yes	n/a	Yes	n/a	Yes	Yes	n/a	Poor vision	Yes	n/a	n/a
Movement disorders	n/a	n/a	n/a	Yes	n/a	Yes	n/a	Gaze deviations	n/a	Gaze deviations	n/a	Yes	No	No	n/a	n/a
Contractures	n/a	n/a	n/a	n/a	n/a	n/a	n/a	n/a	n/a	n/a	n/a	Yes	No	Scoliosis	n/a	No
Cortex	Dysgyria	Dysgyria	Dysgyria	Dysgyria	Dysgyria	Dysgyria	Dysgyria	Dysgyria	Dysgyria	Dysgyria	Dysgyria	Dysgyria	Dysgyria	Dysgyria	Dysgyria	Dysgyria
Bilateral	Yes	Yes	Yes	Yes	Yes	Yes	Yes	Yes	Yes	Yes	Yes	Yes	Yes	Yes	Yes	Yes
Diffuse			Yes				n/a			Yes	Yes				n/a	n/a
A>P gradient	Yes	Yes		Yes	Yes	Yes	n/a	Yes	Yes			Yes	Yes	Yes	n/a	n/a
Perisylvian	Affected	Affected	Affected	Affected	Affected	Affected	Affected	Affected	Affected	Affected	Affected	Affected	Affected	Affected	Affected	
Asymmetrical	No	No	No	No	No	No	L>R	No	No	No	No	No	No	No	No	No
White matter	Normal	Reduced	n/a	Reduced	Reduced	n/a	n/a	Reduced	Reduced	Reduced	Reduced	Normal	Reduced	Reduced	n/a	n/a
Ventricles	Normal	Mildly enlarged	n/a	Mildly enlarged	Mildly enlarged	Normal	Enlarged	Enlarged	Moderately enlarged	Enlarged	Enlarged	Mildly enlarged	Enlarged	Enlarged	Enlarged	Enlarged
Periventricular region	Normal	Reduced white matter	n/a	n/a	n/a	n/a	n/a	Reduced white matter	n/a	n/a	n/a	Normal	Reduced white matter			
Corpus callosum	Normal	Normal	Thin	Normal	Normal	Normal	Hypoplastic	Thin	Normal	Normal	Thin	n/a	Hypoplastic	Normal	ACC	Hypoplastic
Basal ganglia	Normal	Normal	Normal	Normal	Normal	Normal	n/a	Mildy dysmorphic	Mildy dysmorphic	Mildy dysmorphic	Mildy dysmorphic	Mildly dysmorphic	Normal	Dysmorphic	Normal	Dysplastic
Brain stem	Normal	Normal	Normal	n/a	n/a	n/a	Normal	Normal	Normal	Normal	Normal	n/a	Abnormal myelination	Normal	Normal	Normal
Cerebellum	Normal	Normal	Normal	n/a	n/a	n/a	Mildly enlarged	Normal	Normal	Normal	Normal	Normal	Normal	Normal	Enlarged	Hypoplastic
Hippocampus	Normal	Normal	n/a	Normal	Abnormal	Normal	Normal	Abnormal	Normal	Normal	Thin leaves	Normal	Dysmorphic	Normal	Normal	Dysmophic
Other features																Operculation of sylvian fissure, enlarged subarachnoid spaces

b. Supplementary table 2 – Clinical and imaging features of patients with variants in *GRIN2B*

	Platzer et al. 2017	Platzer et al. 2017	Platzer et al. 2017	Platzer et al. 2017	Platzer et al. 2017	Platzer et al. 2017	P5 (This paper)	P6 (This paper)	P7 (This paper)
Pathogenic variant	c.1907C>T, p(Ala636Val)	c.1916C>T, p.(Ala639Val)	c.1963A>T, p.(Ile655Phe)	c.2079A>T, p.(Arg693Ser)	c.2430C>A, p.(Ser810Arg)	c.2429G>A, p.(Ser810Asn)	c.2437C>G, p.(Leu813Val)	c.2438T>C, p.(Leu813Pro)	c. 2453T>C, p.(Met818Thr)
Microcephaly	Yes	n/a	Yes	n/a	Yes	n/a	- 3.2 SD	- 2.2 SD	- 3.9 SD
Development	Severe delay	Severe delay	Severe delay	Severe delay	Severe delay	Severe delay	Severe delay	Severe delay	Severe delay
Neurology							Truncal hypotonia, limb hypertonia	Truncal hypotonia, limb hypertonia, pseudobulbar palsy	Hypertonia
Onset of seizures							4 M	2 Y 3 M	10 W
Type of seizures	Focal seizures, epileptic spasms	Focal and generalized seizures	Generalized seizures, epileptic spasms	Generalized and focal seizures, epileptic spasms	Focal seizures	Generalized seizures, epileptic spasms	Epileptic spasms	GTC with fever	Rapid and rolling eye movements
Cortical visual impairment	Yes	Yes	Yes				No but strabism	Yes	n/a
Movement disorders							No		
Contractures							No		
Cortex	Dysgyria	Dysgyria	Dysgyria	Dysgyria	Dysgyria	Dysgyria	Dysgyria	Dysgyria	Dysgyria
Bilateral	Yes	Yes	Yes	Yes	Yes	Yes	Yes	Yes	Yes
Diffuse	Yes	Yes	Yes	Yes	Yes	Yes	Yes		
A>P gradient								Yes	Yes
Perisylvian	Affected	Affected	Affected	Affected	Affected	Affected	Affected	Affected	Affected
Asymmetrical	No	No	No	No	No	No	No	No	Yes, left > right
White matter	Affected	Affected	Affected	Affected	Affected	Affected	Occipitally reduced	Reduced	Reduced
Ventricles	n/a	Severely enlarged	Mildly enlarged	Enlarged	Severely enlarged	Severely enlarged	Colpocephaly	Enlarged	Enlarged (left)
Periventricular region	n/a	Normal	Normal	Normal	Normal	Normal	Normal	Normal	Normal
Corpus callosum	Normal	Hypoplastic	Normal	Normal	Hypoplastic	Hypoplastic	Hypoplastic	Normal	Dysmorphic
Basal ganglia	Dysmorphic	Dysmorphic	Dysmorphic	Dysmorphic	Dysmorphic	Dysmorphic	Enlarged	Normal	Dysmorphic
Brain stem	Normal	Normal	Normal	Normal	Normal	Normal	Normal	Normal	Normal
Cerebellum	Normal	Normal	Normal	Normal	Normal	Normal	Normal	Normal	Normal
Hippocampus	Dysplastic	Dysplastic	Dysplastic	Normal	Dysplastic	Normal	Normal	Dysmorphic	Normal

c. Supplementary table 3. Abnormal brain MRI findings in NMDAR MCD patients.

	This series		**Cases reported in the literature**	
MRI	GRIN1	GRIN2B	GRIN1	GRIN2B
Dysgyria	4/4	3/3	12/12	6/6
Bilateral	4/4	3/3	12/12	6/6
Diffuse	0/2	2/3	3/11	6/6
A>P Gradient	2/2	2/3	8/11	0/6
Perisylvian fissure	3/3	3/3	12/12	6/6
Asymmetry	0/4	1/3	1/12	0/6
White matter	2/2	3/3	7/9	6/6
Lateral ventricles	4/4	3/3	9/11	5/5
Corpus callosum	3/4	1/3	4/11	3/6
Basal ganglia	2/4	2/3	4/10	6/6
Brainstem	1/4	0/3	0/8	0/6
Cerebellum	2/4	0/3	1/9	0/6
Hippocampus	2/4	1/3	3/11	4/6

Abbreviations: A>P, anterior-to-posterior gradient with anterior regions more affected by dysgyria

2. **Molecular data**

a. **Supplementary table 4**. ACMG-AMP criteria used to classify the NMDAR variants.

Gene	Mutation	ACMG-AMP Criteria	Classification
GRIN1	p.(Tyr474*)	PM2, PVS1, PM3_supporting	Pathogenic
GRIN1	p.(Ser553Leu)	PM2, PP2, PP3, PS2_strong, PM1	Pathogenic
GRIN1	p.(Ala653Thr)	PM2, PP2, PP3, PS2_moderate, PM1	Likely pathogenic
GRIN1	p.(Asp658Tyr)	PM2, PP2, PP3, PS2_moderate, PM1	Likely pathogenic
GRIN1	p.(Cys744Tyr)	PM2, PP2, PP3, PS2_moderate, PM1, PS3_moderate	Likely pathogenic
GRIN2B	p(Leu813Val)	PM2, PP2, PP3, PM5, PS2_moderate, PM1	Likely pathogenic
GRIN2B	p.(Leu813Pro)	PM2, PP2, PP3, PM5 PS2_moderate, PM1	Likely pathogenic
GRIN2B	p.(Met818Thr)	PM2, PP2, PP3, PS2_strong, PM1	Pathogenic

b. Supplementary table 5. *In silico* predictions for the NMDAR missense variants and the homozygous *GRIN1* variants

Gene	*GRIN1*	*GRIN1*	*GRIN1*	*GRIN1*	*GRIN2B*	*GRIN2B*	*GRIN2B*	*GRIN1*
Mutation (NM_007327.3, NM_000834.3)	c.1658C>T, p.S553L	c.1972G>T, p.D658Y	c.1957G>A, p.A653T	c.2231G>A, p.C744Y	c.2437C>G, p.L813V	c.2438T>C, p.L813P	c.2453T>C, p.M818T	c.1422C>A, p.Y474*
Genomic position (hg19)	chr9:g.140056649C>T	chr9:g.140057150G>T	chr9:140057135G>A	chr9:g.140057680G>A	chr12:g.13720120G>C	chr12:g.13720119A>G	chr12:g.13720104A>G	chr9:140055823C>A
SIFT	0.001 Damaging	0 Damaging	0.001 Damaging	0 Damaging	-	-	-	-
Polyphen2 (HDIV)	1 Probably damaging	1 Probably damaging	1 Probably damaging	1 Probably damaging	1 Probably damaging	1 Probably damaging	0.999 Probably damaging	-
Polyphen2 (HVAR)	1 Probably damaging	1 Probably damaging	1 Probably damaging	1 Probably damaging	0.999 Probably damaging	1 Probably damaging	0.999 Probably damaging	-
LRT	0 Unknown	0 Deleterious	0 Deleterious	0 Deleterious	0 Deleterious	0 Deleterious	0 Deleterious	0 Unknown
MutationTaster	1 Disease causing	1 Disease causing	1 Disease causing	1 Disease causing	1 Disease causing	1 Disease causing	1 Disease causing	-
MutationAssessor	3.415 Medium	2.645 Medium	3.21 Medium	3.91 High	3.085 Medium	3.23 Medium	2.395 Medium	-
FATHMM	2.01 Tolerable	0.55 Tolerable	-0.32 Tolerable	0.51 Tolerable	-	-	-	-
PROVEAN	-5.03 Damaging	-6 Damaging	-3.35 Damaging	-9.82 Damaging	-	-	-	-
VEST3	0.899 Damaging	0.574 Damaging	0.749 Damaging	0.99 Damaging	0.851 Damaging	0.981 Damaging	0.935 Damaging	-
MetaSVM	-0.447 Tolerable	-0.328 Tolerable	0.018 Damaging	0.227 Damaging	0.106 Damaging	0.257 Damaging	-0.36 Tolerable	-
MetaLR	0.202 Tolerable	0.34 Tolerable	0.486 Tolerable	0.473 Tolerable	0.503 Damaging	0.547 Damaging	0.329 Tolerable	-
M_CAP	0.425 Damaging	0.914 Damaging	0.823 Damaging	0.48 Damaging	0.606 Damaging	0.919 Damaging	0.551 Damaging	-
CADD	32 Damaging	26.7 Damaging	28.1 Damaging	28.4 Damaging	25.4 Damaging	28.2 Damaging	26 Damaging	36 Damaging
DANN	0.999 Damaging	0.995 Damaging	0.999 Damaging	0.997 Damaging	0.998 Damaging	0.999 Damaging	0.994 Damaging	0.995 Damaging
FATHMM_MKL	0.937 Damaging	0.96 Damaging	0.944 Damaging	0.955 Damaging	0.974 Damaging	0.985 Damaging	0.985 Damaging	0.283 Tolerable
Eigen	0.578 Damaging	0.604 Damaging	0.623 Damaging	0.874 Damaging	0.638 Damaging	0.868 Damaging	0.807 Damaging	-0.385 Tolerable
GenoCanyon	1 Damaging	1 Damaging	1 Damaging	1 Damaging	1 Damaging	1 Damaging	1 Damaging	1 Damaging
fitCons	0.598 Tolerable	0.658 Tolerable	0.658 Tolerable	0.652 Tolerable	0.554 Tolerable	0.554 Tolerable	0.554 Tolerable	0.598 Tolerable
GERP	3.83 Conserved	3.63 Conserved	3.63 Conserved	4.97 Conserved	4.54 Conserved	5.43 Conserved	5.43 Conserved	-3.09 Nonconserved
phyloP	5.468 Conserved	9.153 Conserved	9.582 Conserved	9.314 Conserved	5.025 Conserved	9.32 Conserved	9.32 Conserved	-1.601 Nonconserved
phastCons	1 Conserved	1 Conserved	1 Conserved	1 Conserved	1 Conserved	1 Conserved	1 Conserved	0.0001 Nonconserved
SiPhy	14.305 Conserved	12.526 Conserved	12.526 Conserved	16.773 Conserved	14.17 Conserved	15.484 Conserved	15.484 Conserved	10.605 Nonconserved
REVEL	0.655 Damaging	0.469 Damaging	0.676 Damaging	0.776 Damaging	0.61 Damaging	0.855 Damaging	0.781 Damaging	-
ReVe	0.888 Damaging	0.721 Damaging	0.869 Damaging	0.98 Damaging	0.893 Damaging	0.988 Damaging	0.96 Damaging	0.416 Tolerable
ClinPred	0.97518684 pathogenic	0.99884295 pathogenic	0.99699389 pathogenic	0.9999705 pathogenic	0.98702520 pathogenic	0.99549469 pathogenic	0.99139735 pathogenic	-

Derived from Varcards http://159.226.67.237/sun/varcards/

3. Functional evaluation of a human glutamate receptor variant p.Cys744Tyr in *GRIN1 in vitro*

a. Methods

cDNA Plasmid Constructs: The p.Cys744Tyr and the p.Ala653Thr *GRIN1* variants were introduced into a GluN1 cDNA (RefSeq NM.007327.3) plasmid construct , and the p.Ala653Thr *GRIN2B* variant into the GluN2B cDNA (RefSeq NM_000834.3) via a Quikchange (Agilent) mutagenesis protocol. All experiments used cDNAs encoding human gene sequences verified with Sanger sequencing (Eurofins). mRNA was synthesized from cDNA using mMESSAGE mMACHINE (Invitrogen).

mRNA Injections: The cRNAs for GluN1-C744Y, GluN1-A653T or GluN1-WT were combined, separately, with human GluN2A-WT cRNA, or GluN1-WT and GluN2B-M818T were combined separately, and injected into stage V and VI oocytes and incubated at 16 C for 2–7 days in Barth's culture medium containing (in mM): 88 NaCl, 2.4 $NaHCO_3$, 1 KCl, 0.33 $Ca(NO_3)_2$, 0.41 $CaCl_2$, 0.82 $MgSO_4$, and 10 HEPES (pH 7.4). For experiments, oocytes were removed from the incubator and perfused in recording Barth's solution for two-electrode voltage clamp (TEVC) electrophysiological recordings. Conditions for each experiment are below.

L-Glutamate dose response studies: The recording solution for these studies contained (in mM): NaCl (90), KCl (1.0), $BaCl_2$ (0.5), HEPES (10), and EDTA (0.01), adjusted to pH 7.4 (at 23 degrees C) with NaOH. The oocyte membrane potential was clamped at -40 mV. After a steady baseline was obtained, oocytes were perfused with increasing concentrations of L-glutamate (seven concentrations selected from 0.003, 0.01, 0.03, 0.1, 0.3, 1, 3, 10, 30, and 100 μM) for 0.75 min duration each in the continuous presence of 100 μM glycine. Results at each L-glutamate concentration were normalized to the maximum receptor activation levels (defined as 100%) and the EC_{50} values obtained by fitting concentration-response data with Equation 1 (below).

Glycine dose response studies: The recording solution for these studies was similar as for the L-glutamate studies. The oocyte membrane potential was clamped at -40 mV. After a steady baseline was obtained, oocytes were perfused with increasing concentrations of glycine (seven concentrations selected from 0.003, 0.01, 0.03, 0.1, 0.3, 1, 3, 10, 30 and 100 μM) for 0.75 min duration each in the continuous presence of 100 μM L-glutamate. Results at each glycine concentration were normalized to the maximum receptor activation levels (defined as 100%) and the EC_{50} values obtained by fitting concentration-response data with Equation 1 (below).

Mg^{2+} dose inhibition studies: The recording solution for Mg^{2+} studies contained (in mM): NaCl (90), KCl (1.0), $BaCl_2$ (0.5), and HEPES (10) adjusted to pH 7.4 (at 23 degrees C) with NaOH. The oocyte membrane potential was clamped at -60 mV. After a steady baseline was obtained, oocytes were maximally activated with 100 μM L-glutamate and 100 μM glycine and were then perfused with increasing concentrations of Mg^{2+} (3, 10, 30, 100, 300, and 1000 μM) in the presence of maximal glutamate and glycine. The current responses to glutamate and glycine at each Mg^{2+} concentration were normalized to the maximum receptor activation levels in the absence of Mg^{2+} (defined as 100%) and the IC_{50} values obtained by fitting concentration-inhibition data with Equation 2 (below).

pH studies: The recording solution for these studies contained (in mM): NaCl (90), KCl (1.0), $BaCl_2$ (0.5), HEPES (10), and EDTA (0.01), adjusted to either pH 6.8 or pH 7.6 (at 23 degrees C) with HCl or NaOH. The oocyte membrane potential was clamped at -40 mV. After a steady baseline was obtained in pH 7.6 recording buffer the oocytes were maximally activated with 100 μM L-glutamate and 100 μM glycine in pH 7.6 buffer. Following a washout period to reestablish baseline, the oocytes were then maximally activated with 100 μM L-glutamate and 100 μM glycine in pH 6.8 buffer. The percent current at pH 6.8 was then determined compared to the current at pH 7.6 (defined as 100%).

Zn^{2+} dose inhibition studies: Oocytes expressing recombinant human glutamate receptors were perfused with recording solution containing (in mM): NaCl (90), KCl (1.0), $BaCl_2$ (0.5), Tricine (10), and HEPES (10) adjusted to pH 7.3 (at 23 degrees C) with NaOH. The oocyte membrane potential was clamped at -20 mV. After a steady baseline is obtained, oocytes were maximally activated with 50 μM L-glutamate and 50 μM glycine, and then in the continuous presence of maximal glutamate and glycine, were perfused with increasing concentrations of Zn^{2+} (1, 3, 10, 30, 100, and 300 nM). . Results at each Zn^{2+} concentration are normalized to the maximum receptor activation levels without Zn^{2+} (defined as 100%) and IC_{50} values obtained by fitting concentration-inhibition data with Equation 2 (below).

β-Lactamase Assay: HEK cells were plated in 96-well plates and transiently transfected with cDNA encoding GluN2A-WT and β-lac-GluN1-WT or β-lac-GluN1-C744Y or β-lac-GluN1-A653T. Eight wells were transfected with surface and total expression activities measured in 4 wells each 24 hr post transfection. The ratio of surface (unlysed cells) to total (lysed cells) β-lactamase expression was measured for the β-lac- GluN1-C744Y and β-lac- GluN1-A653T compared to β-lac-GluN1-WT. See PMID 27839871 for further information.

Equation 1: Response = $100 / ((1 + EC_{50} / [agonist])^{nH})$ where EC_{50} is the agonist concentration that elicited the half maximal response, and nH is the Hill slope.

Equation 2: Response = $(100 - minimum) / (1 + ([concentration] / IC_{50})^{nH}) + minimum$ where minimum is the residual percent response in saturating concentration (constrained to ≥ 0) of the experimental compounds, IC_{50} is the concentration of inhibitor that causes half maximal inhibition, and nH is the Hill slope.

Statistical comparisons: For analysis of the IC_{50} or EC_{50} results, the log values of the IC_{50}'s or EC_{50}'s were used for comparison. If the 95% confidence intervals of WT and variant results for each assay do not overlap, a fold effect was then calculated with positive and negative fold values indicating increased or decreased effect on receptor activity, respectively, for that assay measurement.

b. Results

Measurement	GluN1-WT/ GluN2A-WT Mean	95% CI	n	GluN1-**C744Y**/ GluN2A-WT Mean	95% CI	n	Fold Effect on NMDAR[C]
Glutamate EC_{50}, μM	4.0	(3.6, 4.5)	12	1.1	(0.9, 1.3)	12	**3.8**
Glycine, EC_{50}, μM	1.3	(1.1, 1.5)	10	0.7	(0.61, 0.86)	12	**1.8**
Mg^{2+}, IC_{50}, μM	17	(13, 21)	10	29	(21, 38)	12	**NE**
Proton, % [A]	44	(40, 49)	12	74	(68, 81)	12	**1.7**
Zinc, IC_{50}, nM	12	(6.8, 21.9)	10	16	(9.7, 27)	12	**NE**
Zinc, % residual (Ymin) [B]	28	(18, 37)	10	52	(42, 63)	12	**1.9**
Surface/Total Expression %WT	100	(78,122)	4	68	(58,77)	4	**-1.4**
Total Expression %WT	100	(84,116)	4	150	(133,166)	4	**1.5**

Measurement	GluN1-WT/ GluN2A-WT Mean	95% CI	n	GluN1-**A653T**/ GluN2A-WT Mean	95% CI	n	Fold Effect on NMDAR[C]
Glutamate EC_{50}, μM	3.2	(2.9, 3.5)	15	0.12	(0.10, 0.15)	14	**26.4**
Glycine, EC_{50}, μM	1.1	(0.9, 1.2)	15	0.024	(0.019, 0.032)	11	**44.6**
Mg^{2+}, IC_{50}, μM	24	(18, 32)	12	23	(17, 31)	12	**NE**
Proton, % [A]	46	(41, 50)	12	88	(85, 91)	11	**1.9**
Zinc, IC_{50}, nM	6.5	(5.5, 7.7)	12	46	(32, 66)	12	**7.1**
Zinc, % residual (Ymin) [B]	28	(24, 32)	12	67	(57, 75)	12	**2.4**
Surface/Total Expression %WT	100	(92,108)	4	111	(95,127)	4	**NE**
Total Expression %WT	100	(95,105)	4	126	(111,141)	4	**1.2**

Measurement	GluN1-WT/ GluN2B-WT Mean	95% CI	n	GluN1-WT/ GluN2B-**M818T** Mean[D]	95% CI	n	Fold Effect on NMDAR[C]
Glutamate EC_{50}, μM	1.0	(0.9, 1.2)	19	0.42	(0.30, 0.58)	19	**2.5**
Glycine, EC_{50}, μM	0.29	(0.26, 0.33)	20	0.13	(0.097, 0.199)	17	**2.2**
Mg^{2+}, IC_{50}, μM	29	(19, 42)	26	22	(14, 37)	28	**NE**
Proton, % [A]	14	(11, 16)	12	37	(27, 47)	14	**2.7**
Zinc, IC_{50}, nM	not done	-	-	not done	-	-	**-**
Zinc, % residual (Ymin) [B]	not done	-	-	not done	-	-	**-**
Surface/Total Expression %WT	not done	-	-	not done	-	-	**-**
Total Expression %WT	not done	-	-	not done	-	-	**-**

A: % current remaining measured at pH 6.8 compared to pH 7.6 at maximal L-glutamate and glycine activation

B: Current remaining after maximum inhibition by zinc, i.e., the residual current remaining.

C: Fold effect only calculated if 95% CI's do not overlap. Positive and negative fold effects represent gain of function or loss of function effects, respectively, for the parameter measured. NE = no effect.

n= the number of oocytes evaluated for the measured endpoint; CI = confidence interval.

D: Results for GluN2B-M818T reported here are new data and are in line with results reported previously (Platzer et al., J Med Genet 2017;54:460–70).

4. Neuropathological and immunohistochemical studies

a. Morphological studies

A complete autopsy was performed in the two foetuses (individuals 3 and 4) and one neonate (individual 8) following standardized protocols. Fetal biometric data were evaluated according to Guilhard-Costa et al. (2002). The brains were fixed in a 10% formalin-zinc buffer solution for at least one month. Brain growth and macroscopic assessment of brain maturation including gyration were evaluated according to the criteria of Guihard-Costa and Larroche and the atlas of Feess-Higgins and Larroche (1990, 1987). Eight-micrometer sections obtained from paraffin-embedded tissues were stained using Haematoxylin-Eosin. Immunohistochemical procedures included a microwave pre-treatment protocol to aid antigen retrieval (pre-treatment CC1 kit, Ventana Medical Systems Inc, Tucson AZ). Incubations with the primary antibodies listed in supplementary Table 1 were performed for 32 or 44 minutes at room temperature using the Ventana Benchmark XT system. After incubation, slides were processed by means of the Ultraview Universal DAB detection kit (Ventana). A comparative semi-quantitative analysis of immunolabellings in the germinative and intermediate zones as well as in the different layers of the frontal cortex of affected and control patients was assessed and evaluated as follows: 0: no cell labelled; +: very few cells labelled; ++: moderate density of immunolabelled cells and +++: high density of immunolabelled cells.

b.

Supplementary table 6: Antibodies used for the study				
Neural stem cells and progenitors				
Antisera	Cells	Company	Dilution	target
Ki67	Proliferating cells	Agilent	1 :100	Cell cycle related protein
PAX6	Neuroepithelium vRGC, oRGC	Protein Tech group	1 :50	Stem cell transcription factor
SOX2	vRGC, oRGC	Abcam	1 :150	Stem cell self-renewal transcription factor
Ganglionic eminence and cortical interneurons				
GABA	Interneurons	Invitrogen	1:100	Neurotransmitter
Calretinin	Cortical interneurons	Life technology	1:100	Calcium binding protein Cortical interneurons
Post-mitotic neurons and layer markers				
MAP2	Migrating neurons Layers III and V	Sigma Aldrich	1:100	Brain microtubule-associated protein
SATB2	Layers II-IV	Abcam	1:20	Special AT-rich sequence-binding protein
CTIP2	Layers V-VI	Abcam	1:100	COUP-TF-interacting protein 2C2H2 zinc finger transcription factor
vRGC: ventricular radial glial cells; oRGC: outer radial glial cells;				

c.

Supplementary table 7: comparative semi-quantitative analysis of immunolabelling in the germinative and intermediate zones as well as in the different layers of the frontal cortex of affected and control patients

Antibodies	Fœtus 1 25 WG	Control 25 WG	Fœtus 2 30 WG	Control 30 WG	Patient 3 38 WG, dead at postnatal day 6	Control 39 WG
PAX6	++ LGE	+++ LGE	0	0	0	0
SOX2	++ LGE	+++ LGE	++ LGE + SVZ	+++ SVZ +++ LGE	NA	++ VZ
Ki67	+ LGE	++ LGE	+++ LGE + SVZ	++ LGE +++ OSVZ	0	0
GABA	0 LGE + IZ + under the CP	+++ LGE +++ VZ, SVZ, ++ CP	+ LGE and SVZ + Superficial micropolygyric CP	++ diffuse CP	+ in layer II and III	++ all layers
Calretinin	0 LGE and VZ + Layer I (Cajal Retzius cells) 0 in micropolygyric CP Dispersed in nodules	+ IZ + VZ + LGE	+ LGE + superficial micropolygyric CP + IZ +++ nodules	+ VZ + LGE ++ Layers II, III and V	Fibre network layer I + interneurons layer II	++ layers II and III
MAP2	Periventricular nodules + Migrating neurons in IZ 0 CP	+++ VZ Layers III and V	+ micropolygyric CP Dysmorphic neurons	++ layer II and III +++ layer V	+ Immature neurons	++ layers III and V
SATB2	Immature neurons in layer II	+ VZ and LGE ++ IZ +++ diffuse CP	0	Layers II-IV +++ in layer II	0	Layers II-IV, +++ in layer II
CTIP2	0	+++ VZ and LGE +++ prospective layer V	0	++ layer V	0	++ layers V and VI

WG: weeks of gestation; VZ: germinative zone of the dorsal telencephalon; SVZ subventricular zone; LGE: lateral ganglionic eminences; IZ: intermediate zone; CP: cortical plate

d. Supplementary figure 1: Main brain macroscopic and histological findings of individual 8

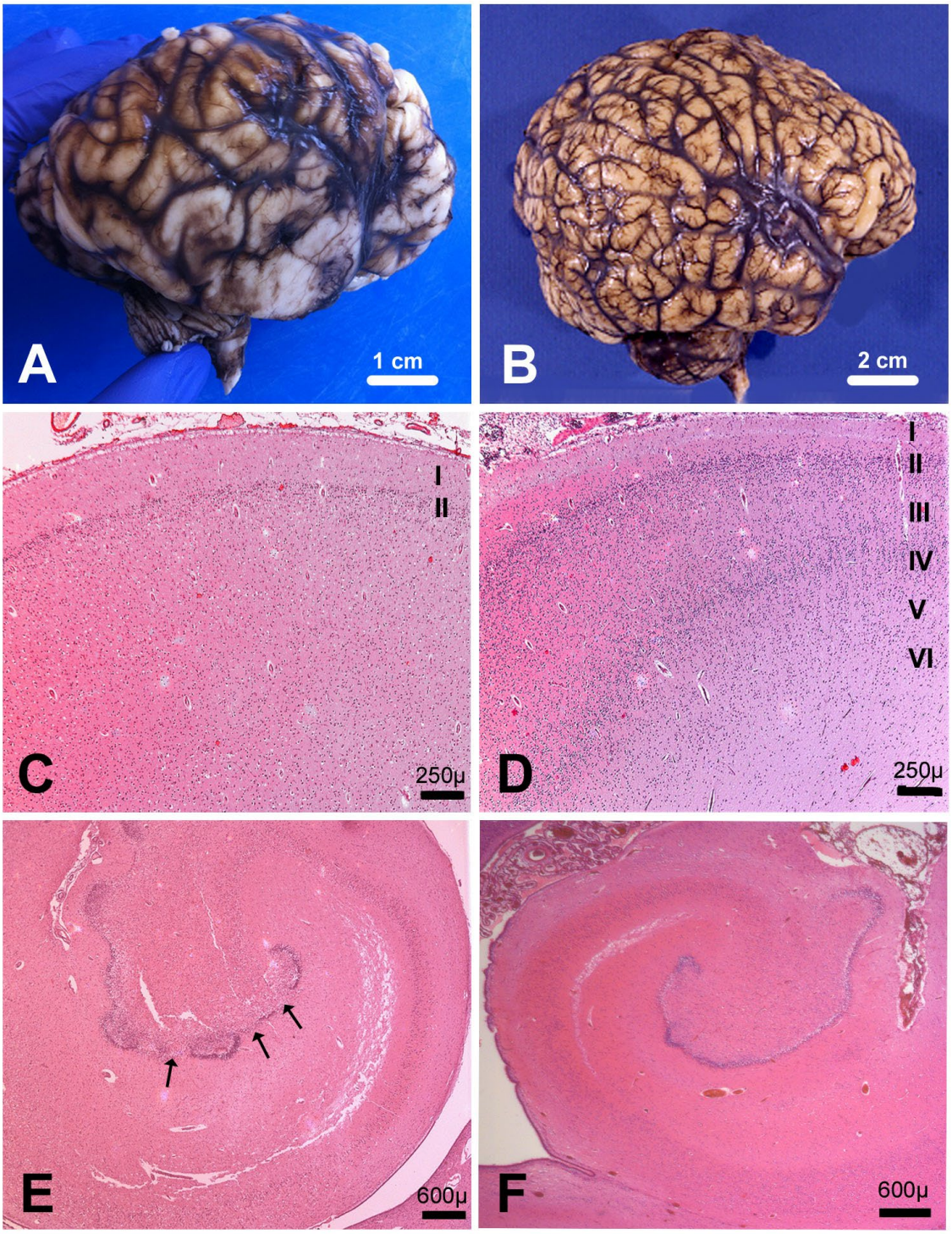

A) Macroscopic view of right side of the neonate brain displaying delayed gyration with no tertiary gyri, broadened sulci and frontal lobe hypoplasia,

B) compared to an age matched control brain, where the tertiary sulcation is in place.

C) Histological view of the temporal cortex in which neuron depletion and dyslamination are observed underneath layer II [H&E, OM x 50],

D) compared with the six-layered cortex of an age-matched control temporal cortex [same OM].

E) Histological view of the hippocampus showing an irregular and fragmented dentate nucleus (arrows), contrasting with a preserved pyramidal cell layer [H&E, OM x 50],

F) compared with a normal hippocampus at the same age [H&E, OM x 50].